J Neurooncol
DOI 10.1007/s11060-008-9659-5

Radiobiologic response of medulloblastoma cell lines: involvement of β-catenin?

Roberta Salaroli · Tiziano Di Tomaso · Alice Ronchi · Claudio Ceccarelli · Silvia Cammelli · Alessandra Cappellini · Giuseppe Nicola Martinelli · Enza Barbieri · Felice Giangaspero · Giovanna Cenacchi

Received: 9 January 2008 / Accepted: 22 July 2008

Abstract Medulloblastoma (MB) is the most common brain malignancy in children. Whole neural axis irradiation is the treatment of choice, but it often results in long-term neurocognitive and developmental impairment. Only insights into MB biology will lead to improved therapeutic outcome. Wingless (WNT) signalling deregulation occurs in up to 25% of sporadic tumors, but the specific role of nuclear β-catenin and its involvement in the radioresponse remains unsettled. Therefore we studied the γ-radiation response of two MB cell lines from cellular and molecular points of view. Our data show that the p53 wild-type cell line is more sensitive to ionizing radiations (IR) than the p53 mutated line, but apoptosis is also induced in p53-mutated cells, suggesting an alternative p53-independent mechanism. In addition, this study is the first to demonstrate that γ-rays trigger the WNT system in our in vitro models. Further studies are required to test if this could explain the radiosensitivity of MB and the favorable prognostic value of nuclear β-catenin in this tumor.

Keywords β-catenin · Cell lines · Ionizing radiation · Medulloblastoma · p53 · Wingless (WNT) signalling

R. Salaroli · T. Di Tomaso · A. Ronchi · C. Ceccarelli · S. Cammelli · G. N. Martinelli · E. Barbieri · G. Cenacchi (✉)
Dipartimento Clinico Scienze Radiologiche e Istocitopatologiche, "Alma Mater" Università di Bologna, Bologna, Italy
e-mail: giovanna.cenacchi@unibo.it

A. Cappellini
Dipartimento Scienze Morfologiche, "Alma Mater" Università di Bologna, Bologna, Italy

T. Di Tomaso
Dipartimento Scienze Biomediche Comparate, Università di Teramo, Teramo, Italy

F. Giangaspero
Dipartimento di Medicina Sperimentale, Università "La Sapienza", Rome, Italy

F. Giangaspero
IRCSS Neuromed, Pozzilli, IS, Italy

Introduction

Medulloblastoma (MB) is the most common malignant brain tumor in children [1–3]. The usual therapy for MB consists in maximal tumor resection followed by whole neural axis irradiation and chemotherapy. Although advances in treatment regimens have improved the 5-year survival rates to ~70% for average-risk and to 25% for high-risk patients, both groups are still associated with substantial mortality. Radiation is a highly effective therapy for MB, but it causes severe damage to the developing brain. Therefore, further improving the outcome for children with MB remains an important objective for physicians and scientists. There is a general consensus that a greater understanding of MB biology and the molecular mechanisms underlying the cellular response to IR will improve the way existing therapies are used [4]. Among the various molecular pathways which appear to be involved in MB pathogenesis, wingless (WNT) signalling seems to play an important role, occurring in up to 25% of sporadic MB [5–9]. Canonical WNT signalling induces stabilization and nuclear localization of β-catenin by compromising the ability of a multiprotein complex containing axin, adenomatous polyposis coli (APC) and glycogen synthase kinase 3β (GSK3β) to target it for degradation and block its nuclear import [10]. Nuclear β-catenin interacts with members of the Lymphoid Enhancer Factor-T Cell Factor family of transcription factors, leading to activation of various target genes [5, 11]. On the one hand, it is

emerging that WNT pathway activation may exert disparate effects on cells, potentially in a highly context- or cell-dependent fashion. In fact nuclear β-catenin can promote proliferation and aggressive behavior in some cell systems and apoptosis and/or growth arrest in others [12]. On the other hand, it is known that a range of stimuli can promote WNT activation, but its involvement in the cancer cell response to IR needs to be further investigated since only a few studies have been done [13,14,16,17], and none on MB cell lines.

The purpose of this study was threefold: (1) to investigate the cellular response to IR of MB cell lines, (2) to determine whether IR can modulate the WNT/β-catenin signalling pathway, and (3) to evaluate the existence of an interplay between β-catenin and p53, a key regulator of cellular radioresponse.

Materials and methods

Cell lines and culture conditions

Human MB cell lines (DAOY and D283MED) were obtained from the American Type Culture Collection (ATCC, Manassas, VA). These lines have no mutation of the WNT pathway components but DAOY is p53 mutated, whereas D283MED expresses cellular myelocytomatosis oncogene (c-myc) at high levels, both mRNA and protein [13–15]. The cell lines were maintained as exponentially growing cultures in Eagle's minimum essential medium (EMEM) with Earle's BSS (Invitrogen Corporation; Frederick, MD) supplemented with 20% heat-inactivated foetal bovine serum (FBS, Invitrogen Corporation; Frederick, MD), 1% L-glutamine (Eurobio; Courtaboeuf Cedex, France), 0.5% gentamycin (Euroclone; Life Sciences Division, MI), 0.5% neomycin (Sigma-Aldrich; St. Louis, MO), 1% nonessential amino acids (Eurobio; Courtaboeuf Cedex, France), and 1% sodium pyruvate (Eurobio; Courtaboeuf Cedex, France). Two colon cancer cell lines (from ATCC) were used as controls: RKO with wild-type WNT pathway components and SW480 with a truncated form of APC protein and subsequently an accumulation of nuclear β-catenin [18, 19]. RKO cell line was grown on DMEM (Eurobio; Courtaboeuf Cedex, France) supplemented with 10% heat-inactivated FBS (Invitrogen Corporation; Frederick, MD), 1% L-glutamine (Eurobio; Courtaboeuf Cedex, France), 0.5% gentamycin (Euroclone; Life Sciences Division, MI), 0.5% neomycin (Sigma-Aldrich; St. Louis, MO), and 0.5% nonessential amino acids (Eurobio; Courtaboeuf Cedex, France). SW480 cell line was grown in L15 (Leibovitz Medium, Eurobio; Courtaboeuf Cedex, France) supplemented with 10% heat-inactivated FBS (Invitrogen Corporation; Frederick, MD), 1% L-glutamine (Eurobio; Courtaboeuf Cedex, France), 0.5% gentamycin (Euroclone; Life Sciences Division, MI), 0.5% neomycin (Sigma-Aldrich; St. Louis, MO), and 0.5% nonessential amino acids (Eurobio; Courtaboeuf Cedex, France). Cell cultures were maintained at 37°C in 5% CO_2.

IR treatment

The cells were plated 24 h prior to irradiation with an Irradiateur Biologique 437C (CIS-BIO; Cedex, France) γ-ray machine at a dose of 6 Gy and a dose rate of approximately 2 Gy/min.

Post irradiation, cells were analyzed at different time points to evaluate growth rate, effects on the cell cycle, cell viability, apoptosis induction, β-catenin, c-myc, and p53 expression and localization.

Cell growth analysis

Both treated and untreated cells were seeded in 25 cm^2 flasks at a density of 2×10^5 cell/flask for 24 h; after that, half of the samples were irradiated. Cells were harvested by trypsinization every 24 h for 5 days and counted using a Neubauer chamber. Each count was performed three times.

Cell cycle analysis

Flow cytometric analysis was performed to evaluate cell cycle changes due to the IR treatment at different time points (5, 16, 24, and 48 h). Cells were washed with Phosphate Buffered Saline (PBS), collected after trypsinization, and stained according to Nusse et al. [20]. Briefly, they were centrifuged for 5 min at 233*g*, and then adjusted to a density of 1.2×10^6 cell/ml for D283MED and 4×10^5 cell/ml for DAOY in Nusse lysis solutions. Solution 1 (NaCl 584 mg/l, Na-citrate 1,000 mg/l, RNasi 10 mg/l, Nonidet P40 0.03%) was added and samples were incubated at 4°C. After 30 min the same volume of solution 2 (citric acid 1.5%, sucrose 0.25 M) was added and the samples were stored at 4°C until analysis. DNA staining was carried out using a propidium iodide (PI) solution 50 μg/ml (Sigma-Aldrich; St. Louis, MO) for 30 min at 4°C. Samples were analyzed by means of a flow cytometer (Bryte HS; Biorad, Munich, Germany): cell cycle changes, identified and measured on the PI fluorescence histogram, were evaluated by using ModFit software (Verity Software House; Topsham, ME). The experiments were performed in duplicate for each data point.

Cell viability analysis

The cells were seeded in 25 cm^2 culture flasks and collected 24, 48, and 72 h post IR. At the same time points, untreated cells (controls) were harvested. For viability analysis, cells were trypsinized and resuspended 1:1 in

Trypan Blue solution (Sigma-Aldrich; St. Louis, MO) and counted using a Neubauer chamber. At each time point three flasks were counted to obtain an average value and the experiments were performed in triplicate.

Apoptosis assay

After IR treatment, cells were collected and analyzed at different time points (8, 24, 48, and 72 h) by flow cytometry to evaluate the percentage of apoptotic cells using the Vybrant apoptosis assay kit #4 (Molecular Probes, Invitrogen Corporation; Frederick, MD) according to the manufacturer's instructions. Flow cytometric analyses were performed with a Coulter Epics XL/XL-MCL (Beckman Coulter) equipped with an argon ion laser at 488 nm wavelength and using the System II software. The experiments were performed in triplicate.

Western blot (WB) analysis

Cells were harvested at specific time points (1–6, 8, 16, and 24 h), washed with PBS, and total protein extracts were prepared by dissolving the cell pellets in the following extraction buffer: Triton 1%, glycerol 10%, Tris 50 mM pH 7.4, NaCl 150 mM, ethylene diamine tetraacetic acid (EDTA) 2 mM pH 8.0, $MgCl_2$ 2 mM, and Complete EDTA-Free (Roche Diagnostic, Indianapolis, IN) 2×. After incubation (20 min on ice), cell debris was cleared by centrifugation (13,225*g*, 30 min, 4°C) and the supernatant protein concentration was assessed with Bradford reagent (Biorad Laboratories GmbH; Munich, Germany).

Nuclear proteins were extracted at 5, 8, 16, and 24 h after irradiation. To isolate the nuclear proteins, cells were washed with PBS, collected, and then incubated with five volumes of hypotonic buffer (HEPES 10 mM pH 7.9, $MgCl_2$ 1.5 mM, KCl 10 mM, and Complete EDTA-Free 2×) to remove salts and PBS. The cells were then incubated with two volumes of hypotonic buffer for 10 min on ice. The nuclear pellets were isolated by centrifugation at 827*g* for 15 min at 4°C. The nuclei obtained were rinsed with ½ volume of LOW buffer (HEPES 20 mM pH 7.9, Glycerol 25%, KCl 20 mM, $MgCl_2$ 1.5 mM, EDTA 0.2 mM, Complete EDTA-Free 2×) and ½ volume of HIGH buffer (HEPES 20 mM pH 7.9, glycerol 25%, KCl 1.2 M, $MgCl_2$ 1.5 mM, EDTA 0.2 mM, Complete EDTA-Free 2×) and incubated on ice for 30 min. The protein suspension was centrifuged at 13,225*g* for 30 min at 4°C and the protein concentration of supernatant was determined as described.

Aliquots of nuclear pellets were stained with hematoxylin-eosin (HE) stain and observed under a light microscope (Carl Zeiss GmbH; Germany) to verify the lack of cytoplasmic contamination.

The same amount of proteins was subjected to 10% sodium dodecyl sulfate–polyacrylamide gel electrophoresis (SDS–PAGE) and transferred onto a nitrocellulose membrane (Hybond-C Extra, Amersham Biosciences; Little Chalfont, UK), blocked with blocking solution (5% nonfat dry milk in TBS, 20 mM Tris–HCl, 137 mM NaCl, pH 7.6; 0.1% Tween-20) and incubated in blocking solution containing primary antibodies: rabbit polyclonal anti-β-catenin (H-102, Santa Cruz Biotechnology; Santa Cruz, CA) 1:600, mouse monoclonal anti-p53 (1C12, Cell Signalling Technology; Danvers MA) 1:2,000, mouse monoclonal antibody anti-c-myc (9E10, Santa Cruz Biotechnology; Santa Cruz, CA) 1:100, goat polyclonal anti-β-actin (I-19, Santa Cruz Biotechnology; Santa Cruz CA) 1:1,000, and goat polyclonal anti-Lamin B (C-20, Santa Cruz Biotechnology; Santa Cruz CA) 1:1,000. Membranes were washed to remove unbound antibodies and then probed with horseradish peroxidase (HRP)-labeled secondary antibodies diluted in blocking solution: anti-goat (Santa Cruz Biotechnology; Santa Cruz CA) 1:1,000, anti-rabbit and anti-mouse (Amersham Biosciences; Europe GmbH) 1:10,000. After washing, the HRP activity was detected using an Enhanced chemiluminescence kit (ECL-PLUS, Amersham Biosciences; Europe GmbH) and revealed with Hyperfilm ECL (Amersham Biosciences; Europe GmbH). For all the experiments, β-actin- or Lamin B-normalized immunoblotting data were quantified by densitometry using specific software (Gel-Pro Analyzer, version 3.0; Media Cybernetics, Silver Spring, MD). The experiments were performed in duplicate.

Immunofluorescence

The cells were cultured on glass coverslips for 24 h before irradiation, then fixed at different time points (5, 8, 16, and 24 h) post IR with 2% paraformaldehyde in PBS for immunofluorescence (IF) staining of β-catenin as previously described [21]. The experiments were performed in duplicate.

Statistical analysis

Data were analyzed using the Dunnett test on a graphpad software package for Windows (PRISM). A P value <0.05 was considered as statistically significant.

Results

IR cellular effects

IR treatment induced slightly different responses in D283MED and DAOY cell lines. D283MED cells showed

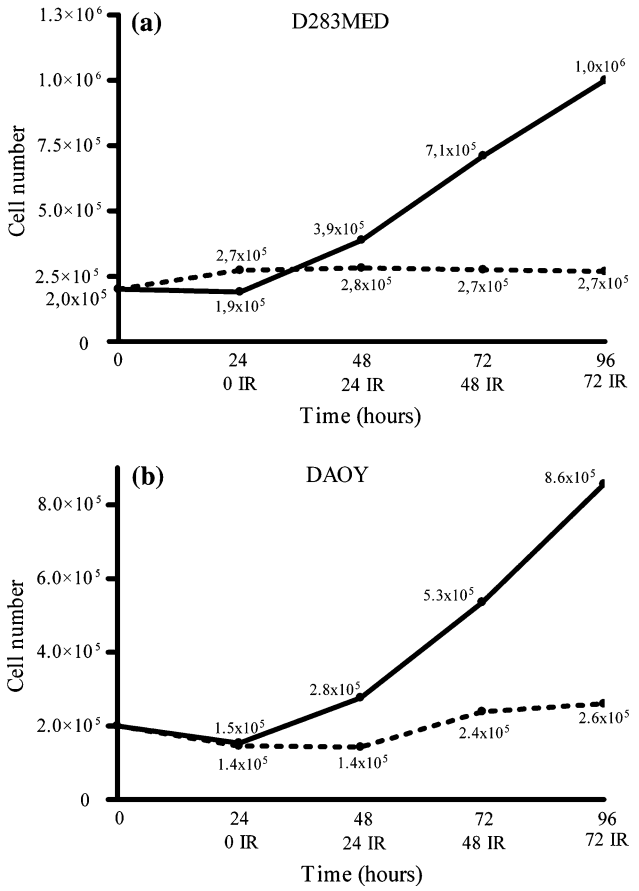

Fig. 1 Cell growth of D283MED (**a**) and DAOY (**b**): IR-treated (dotted line) and control (continuous line). Cells were plated 24 h prior to irradiation. D283MED cells showed growth arrest for 72 h after IR, while in DAOY the growth rate was noticeably slower than in untreated cells

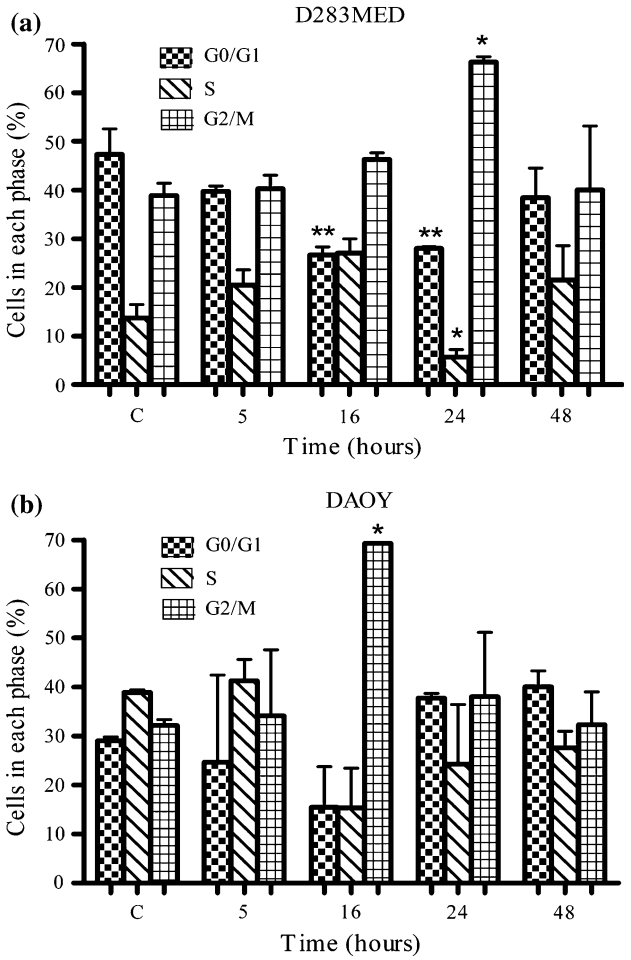

Fig. 2 Cell cycle of D283MED (**a**) and DAOY (**b**) at 5, 16, 24, and 48 h post IR and control (C). Bar charts shows the means of percentages of cells in different cycle phases obtained in two independent experiments. At 24 h post IR D283MED showed a decrease of S phase and accumulation of cells in G2/M; the cell cycle was re-established 24 h after these arrests. DAOY cells showed an arrest only in the G2/M phase 16 h post IR; just 8 h after the cell cycle was re-established. $^{*}P < 0.05$

growth arrest for at least 72 h after IR, while in DAOY the growth rate was noticeably slower than in untreated cells. The doubling time of untreated D283MED and DAOY cells was 37 and 26.5 h, respectively. After irradiation both cell lines showed a doubling time greater than 72 h (Fig. 1). Figure 2 describes the cell cycle progress of D283MED and DAOY cells post IR. At 24 h post IR, D283MED showed a decrease of the S phase with a simultaneous accumulation of cells in G0/G1 and G2/M, whereas after 48 h the cell cycle was re-established. On the contrary, at 16 h post IR, DAOY cells showed arrest only in the G2/M phase. The cell cycle was re-established 24 h post IR. In D283MED cellular viability was significantly decreased, compared with untreated cells, at 48 and 72 h post IR, whereas in DAOY cellular viability was much higher as demonstrated by Trypan blue exclusion assay (Fig. 3a).

Figure 3b shows the fraction of apoptotic cells in both cell lines after the IR treatment. In comparison with untreated cells, D283MED demonstrated a significant percentage of apoptotic cells at 48 and 72 h post IR, while the proportion of apoptotic DAOY cells was statistically significant only at 48 h: an early, but not significant increase in the apoptotic fraction at 24 h post IR can be appreciated.

IR molecular effects

WB analysis of β-catenin and p53 in D283MED cells demonstrated that radiation induced an increase in total β-catenin expression with the highest level observed at 3 h post IR followed by a sharp decrease until steady-state levels. The p53 trend was similar, but with a maximum value observed 5 h post IR. On the contrary, total β-catenin protein levels were only moderately increased compared with untreated cells in DAOY, while p53 levels were

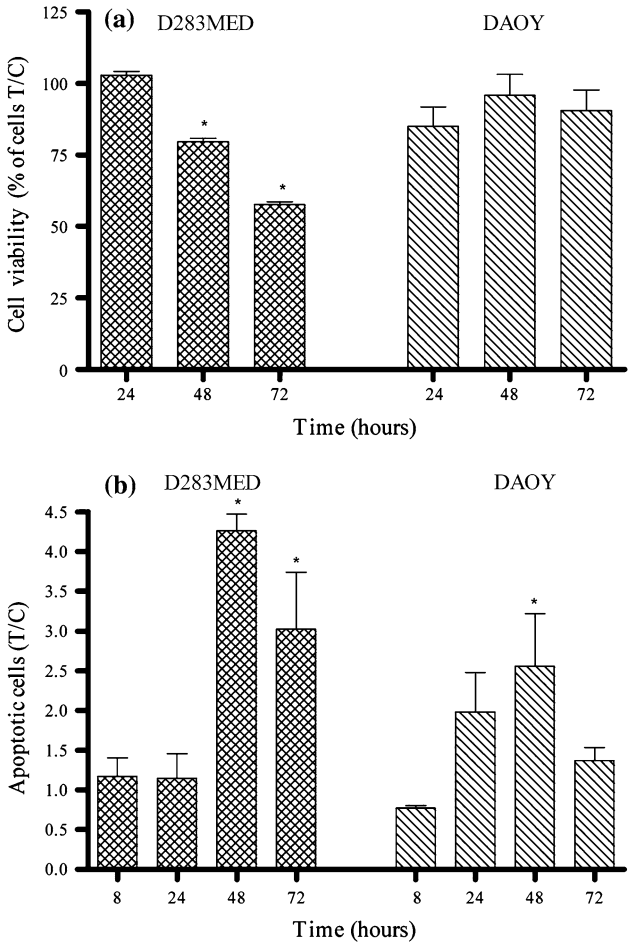

Fig. 3 (**a**) Cell viability of D283MED and DAOY at 24, 48, and 72 h post IR. Percentage of viable cells: 102.88%, 79.66%, 57.63% (D283MED) and 84.95%, 95.88%, 90.46% (DAOY). In D283MED cellular viability was significantly decreased at 48 and 72 h post IR, whereas in DAOY cells viability was not significantly decreased. (**b**) Apoptosis of D283MED and DAOY at 8, 24, 48, and 72 h post IR. Percentage of apoptotic cells: 117%, 115%, 426%, 302% (D283MED) and 77%, 198%, 256%, 137% (DAOY). D283MED demonstrated a significant percentage of apoptotic cells at 48 and 72 h post IR, whereas the proportion of apoptotic DAOY cells was statistically significant only at 48 h. Bar charts show the means of the ratio between treated (T) and relative control (C) samples obtained in three independent experiments. $*P < 0.05$

characterized by a very irregular trend (Fig. 4). A nuclear upregulation of β-catenin protein levels was observed in D283MED at 5 and 16 h post IR, while in DAOY this increase was detectable only at 5 h post IR (Fig. 5).

Subcellular localization of β-catenin was determined by IF analysis, to verify whether the nuclear increase in the β-catenin level after IR corresponded to its translocation. Untreated D283MED cells showed that the cell membranes were strongly reactive for β-catenin mainly at the level of intercellular junctions. No differences were detectable in the D283MED post IR, probably due to the basal low level of β-catenin [21]. Untreated DAOY showed both diffuse membrane and cytoplasmic immunopositivity for β-catenin; β-catenin was evident in the cell nuclei 5, 8, and 24 h post IR (Fig. 6). To examine whether nuclear translocation of β-catenin implied activation of WNT signalling a WB analysis of expression levels of c-myc was performed: there was a large increase in protein expression in each cell line running parallel to increased nuclear β-catenin following IR treatment (Fig. 7).

Discussion

Radiation therapy is commonly accepted as being the cornerstone of successful treatment of MB [3, 4, 22, 23]. For MB patients, whole neural axis radiotherapy can improve survival and reduce recurrence and metastases [24, 25]. However, radiotherapy has considerable side-effects on children's growth, brain development, and behavior [26, 27]. To improve therapeutic outcomes and reduce the toxicity of current treatments a greater understanding of MB biology and of tumor response to IR is needed.

Over the past 15 years, major efforts by many laboratories have focused on the cellular and molecular biology of stress induced by IR [28]. Many of these studies have also attempted to elucidate the transcription factors activated by IR, but only a few researches on MB cell lines' radioresponse have been performed, and none of them have been focused on WNT signalling. We therefore investigated the γ-radiation response of two MB cell lines at both the cellular and molecular level. Cellular radioresponse involves a complex and active process, dependent on numerous genes whose combination determines the final outcome [29–38]. Among these, the tumor suppressor protein p53 is the key determinant of the genotoxic stress response in mammalian cells [30, 31, 34, 39–42]. So we chose the p53-mutated DAOY and the wild-type p53 D283MED as an in vitro model of MB.

After IR treatment, both cell lines showed alterations in cell proliferation, cell cycle, viability, and apoptotic cell death. In particular, D283MED proliferation was inhibited with a growth rate arrest at least for 72 h and viability strongly decreased with statistically significant values at 48 and 72 h, whereas DAOY cells suffered only a slower growth rate without a significant decrease of survival. These effects correlated with an induced p53-dependent arrest of D283MED cells in both G1/S and G2/M at 16 and 24 h post IR. On the contrary, the DAOY cell line showed an early arrest only at G2/M at 16 h post IR with a restart of cell cycling at 24 h. Since apoptosis is an important response to radiation we also analyzed the contribution of apoptotic death to the global IR-induced mortality. The highest percentage of apoptotic cells was

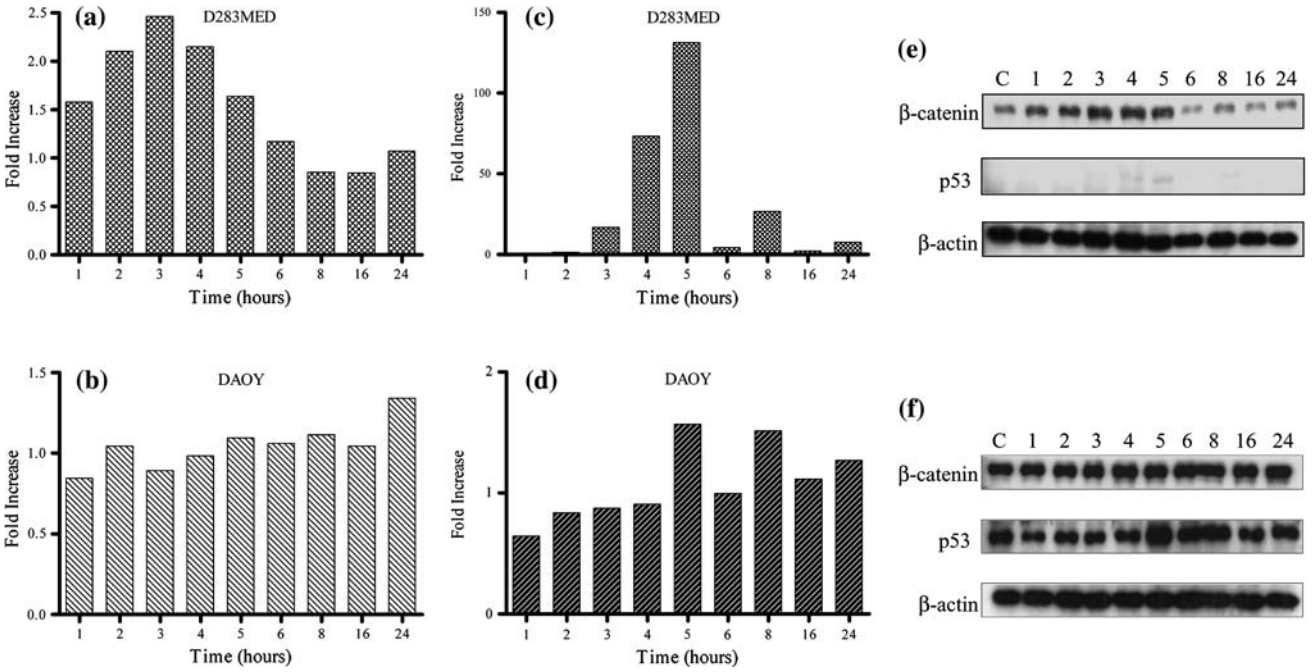

Fig. 4 Total levels of β-catenin and p53 in D283MED (**a**, **c**) and in DAOY (**b**, **d**) at 1–6, 8, 16, and 24 h post-IR. Each sample was normalized with β-actin. Bar charts show the means of the ratios between treated and relative control (C) samples obtained in two independent experiments (fold increase). (**e**, **f**) Representative Western blots. In D283MED we observed an increase in total β-catenin and p53 expression with the highest level of the first one at 3 h post IR and the maximum level of the second one at 5 h post IR; afterwards the two protein levels decreased until steady state. Total β-catenin protein levels were moderately increased compared with untreated cells in DAOY, whereas p53 levels were characterized by a very irregular trend

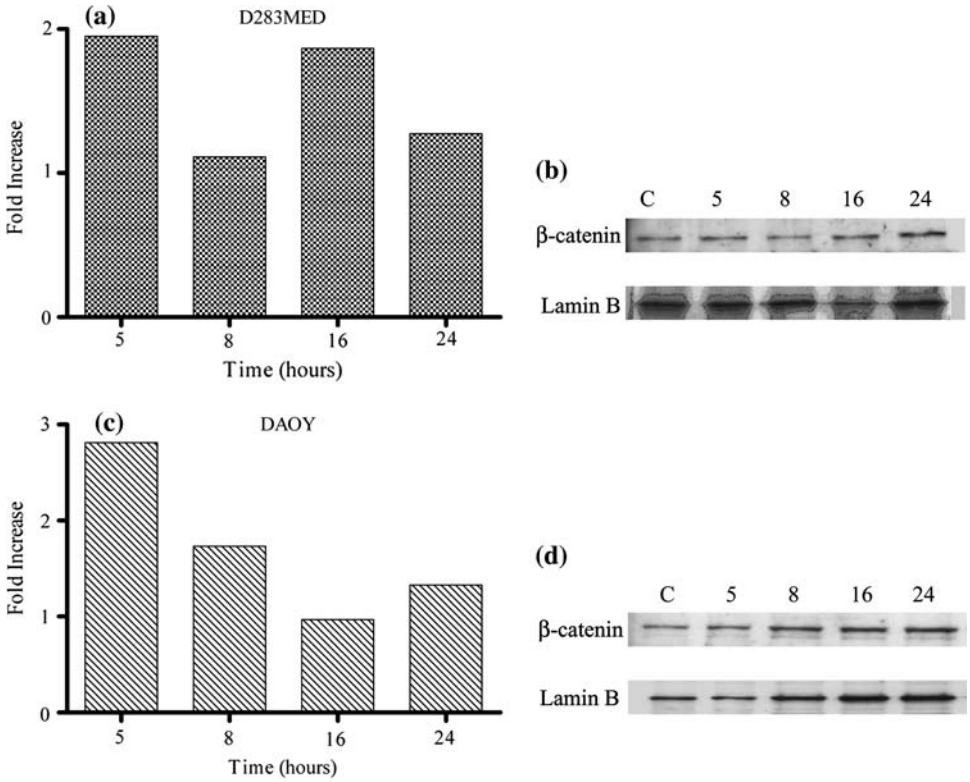

Fig. 5 Nuclear levels of β-catenin in D283MED (**a**) and in DAOY (**c**) at 1–6, 8, 16, and 24 h post IR. Each sample was normalized with Lamin B. Bar charts show the means of ratios between treated and relative control (C) samples obtained in two independent experiments (fold increase). (**b**, **d**) Representative Western blots. An upregulation of nuclear β-catenin was observed in D283MED at 5 and 16 h post IR and in DAOY at 5 h post IR

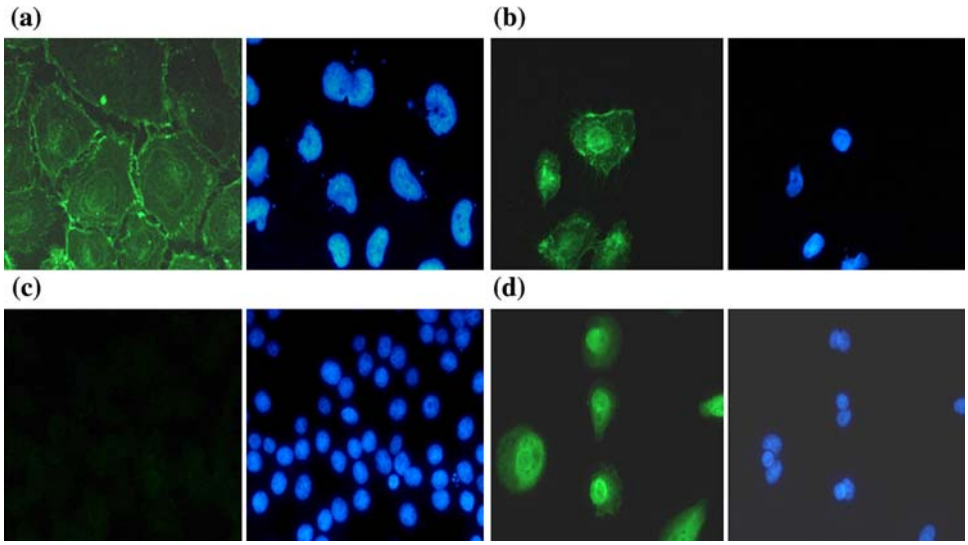

Fig. 6 Localization of β-catenin in untreated (**a**) and treated DAOY (**b**) 5 h post IR. β-catenin was evident in the cell nuclei after treatment. Untreated RKO (**c**) and SW480 (**d**) were used as control cell lines: RKO showed faint membrane immunopositivity while SW480 showed strong nuclear β-catenin reaction. (4′,6-diamino-2-phenylindole-counterstained cell nuclei). 40×

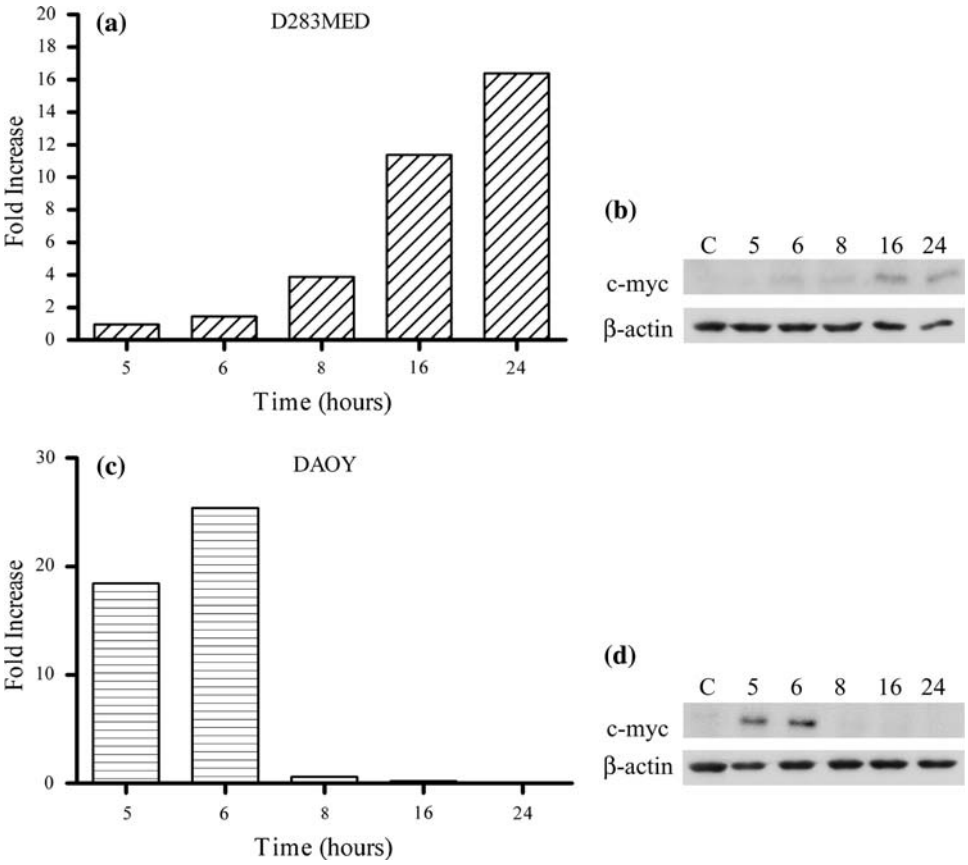

Fig. 7 Levels of c-myc in D283MED (**a**) and in DAOY (**c**) at 1–6, 8, 16, and 24 h post-IR. Each sample was normalized with β-actin. Bar charts show the means of ratios between treated and relative control (C) samples obtained in two independent experiments (fold increase). (**b**, **d**) Representative Western blots. C-myc expression increased in each cell lines after IR treatment, mainly at 16 and 24 h in DAOY and at 5 and 6 h in D283MED

observed at 48 h post IR in both DAOY and D283MED cells with the apoptosis values three times higher in D283MED cells. Altogether these data confirm that the p53 wild-type cell line is more sensitive to γ-rays than the p53 mutated line and support evidence that p53 mutations contribute to the development of aggressive forms of MB [43].

From the molecular point of view we observed a total β-catenin increase following irradiation that is mild and prolonged in time in DAOY, whereas in D283MED it is higher and short-lasting. These differences might be related to a different basal level of β-catenin in MB cell lines (high in DAOY and very low in D283MED) [21] and to the possible absence of a p53-mediated mechanism of β-

catenin degradation in p53-mutated DAOY cells. In this connection, deregulation of β-catenin is known to lead to p53 activation through ARF in many cell lines [39, 44]. On the other hand, accumulation of p53 results in downregulation of β-catenin by enhancing its degradation through GSK3β or the SIAH1 pathway [45, 46]. However, it has not been investigated whether this cross-talk exists in MB cells. In D283MED cells top levels of total β-catenin can be seen before the increase in p53 levels, then both β-catenin and p53 return to basal levels. This could suggest that such a rise in β-catenin levels is sufficient to induce a marked increase in the steady-state levels of p53 and seems to confirm the interplay between the two proteins in our MB cell line. Very interestingly, IR increased nuclear β-catenin levels in both cell lines. IF disclosed that DAOY treated cells had markedly elevated levels of β-catenin in the cell nuclei, whereas control cells retained the typical membranous staining pattern of the protein. This was not observed in D283MED, probably because the low basal levels of β-catenin and the particular morphology of this cell line make this phenomenon difficult to visualize. The increased expression levels of c-myc, a target gene of the TCF-β-catenin pathway, shows that accumulation of β-catenin in the nuclei is accompanied by enhanced transcriptional activity. It has recently emerged that β-catenin may exert disparate effects on cell viability, potentially in a highly context- or cell-dependent fashion. Although β-catenin nuclear accumulation is often associated with enhanced proliferation, several reports link stabilization of β-catenin to apoptosis or to growth arrest [47–53]. Specific experimental models are needed to demonstrate an unequivocal correlation between the cellular response of our MB cell lines and nuclear accumulation of β-catenin. However, these findings are in accordance with previous observations of the involvement of β-catenin in both G2/M and G1/S cell cycle arrest and apoptosis [47–53]. It is noteworthy that γ-radiation induced apoptosis in the p53-mutated cell line, suggesting an alternative signalling pathway. One such pathway could be mediated by the regulation of cellular β-catenin levels.

In conclusion, this is the first study demonstrating that IR triggers activation of WNT signalling in MB cell lines. Further study are however required to verify if this event is associated with the selection of a less aggressive phenotype or a phenotype more sensitive to IR and to explain why MB is considered a radiosensitive tumor. This could also account for the favorable prognostic value of nuclear β-catenin from a molecular point of view [12].

Acknowledgments This research project was partially supported by PRIN 2002 and 2006 and MIUR ex60% grants. We acknowledge L. Montanaro for valuable discussion.

References

1. Eberhart CG, Kepner JL, Goldthwaite PT et al (2002) Histopatologic grading of medulloblastomas: a pediatric oncology group study. Cancer 94:552–560. doi:10.1002/cncr.10189
2. Kleihues P, Luis DN, Scheithauer BW et al (2002) The WHO classification of tumors of the nervous system. J Neuropathol Exp Neurol 61:215–225
3. Ellison D (2002) Classifying the medulloblastoma: insights from morphology and molecular genetics. Neuropathol Appl Neurobiol 28:257–280. doi:10.1046/j.1365-2990.2002.00419.x
4. Gilbertson RJ (2004) Medulloblastoma: signaling a change in treatment. Lancet Oncol 5:209–218. doi:10.1016/S1470-2045(04)01424-X
5. Giangaspero F, Wellek S, Masuoka J et al (2006) Stratification of medulloblastoma on the basis of histopathological grading. Acta Neuropathol 112:5–12. doi:10.1007/s00401-006-0064-x
6. Koch A, Hrychyk A, Hartmann W et al (2007) Mutations of the Wnt antagonist AXIN2 (Conductin) result in TCF-dependent transcription in medulloblastomas. Int J Cancer 121:284–291. doi:10.1002/ijc.22675
7. Eberhart CG, Tuhan T, Burger PC (2000) Nuclear localization and mutation of β-catenin in medulloblastomas. J Neuropathol Exp Neurol 59:333–337
8. Clifford SC, Lusher ME, Lindsey JC et al (2006) WNT/Wingless pathway activation and chromosome 6 loss characterize a distinct molecular sub-group of medulloblastomas associated with a favorable prognosis. Cell Cycle 5:2666–2670
9. Ellison DW, Clifford SC, Gajjar A et al (2003) What's new in neuro-oncology? Recent advances in medulloblastoma. Eur J Paediatr Neurol 7:53–66. doi:10.1016/S1090-3798(03)00014-X
10. Cadigan KM, Liu YI (2006) Wnt signaling: complexity at the surface. J Cell Sci 119:395–402. doi:10.1242/jcs.02826
11. Marino S (2005) Medulloblastoma: developmental mechanisms out of control. Trends Mol Med 11:17–22. doi:10.1016/j.molmed.2004.11.008
12. Ellison DW, Onilude OE, Lindsey JC, United Kingdom Children's Cancer Study Group Brain Tumour Committe et al (2005) β-Catenin status predicts a favorable outcome in childhood medulloblastoma: the United Kingdom Children's Cancer Study Group Brain Tumour Committee. J Clin Oncol 23:7951–7957. doi:10.1200/JCO.2005.01.5479
13. Woodward WA, Chen M, Behbod F et al (2007) WNT/β-catenin mediates radiation resistance of mouse mammary progenitor cells. Proc Natl Acad Sci USA 104:618–623. doi:10.1073/pnas.0606599104
14. Rodningen OK, Borresen-Dale AL, Alsner J et al (2008) Radiation-induced gene expression in human subcutaneous fibroblasts is predictive of radiation-induced fibrosis. Radiother Oncol 86:314–320. doi:10.1016/j.radonc.2007.09.013
15. Siu IM, Lal A, Blakenship JR et al (2003) c-Myc promoter activation in medulloblastoma. Cancer Res 63:4773–4776
16. Gassler N, Herr I, Keith M et al (2004) Wnt-signaling and apoptosis after neoadjuvant short-term radiotherapy for rectal cancer. Int J Oncol 25:1543–1549
17. Chen MS, Woodward WA, Behbod F et al (2007) Wnt/beta-catenin mediates radiation resistance of Sca1+ progenitors in an immortalized mammary gland cell line. J Cell Sci 120:468–477. doi:10.1242/jcs.03348
18. Dihlmann S, Siermann A, von Knebel Doeberitz M (2001) The nonsteroidal anti-inflammatory drugs aspirin and indomethacin attenuate β-catenin/TCF-4 signaling. Oncogene 20:645–653. doi:10.1038/sj.onc.1204123

19. Ricciardiello L, Baglioni M, Giovannini C et al (2003) Induction of chromosomal instability in colonic cells by the human polyomavirus JC virus. Cancer Res 63:7256–7262
20. Nusse M, Beisker W, Hoffmann C et al (1990) Flow cytometric analysis of G1- and G2/M-phase subpopulations in mammalian cell nuclei using side scatter and DNA content measurements. Cytometry 11:813–821. doi:10.1002/cyto.990110707
21. Salaroli R, Russo A, Ceccarelli C et al (2007) Intracellular distribution of beta-catenin in human medulloblastoma cell lines with different degree of neuronal differentiation. Ultrastruct Pathol 31:33–44. doi:10.1080/01913120601169501
22. Jozwiak J, Grajkowska W, Wlodarski P (2007) Pathogenesis of medulloblastoma and current treatment outlook. Med Res Rev 27:869–890. doi:10.1002/med.20088
23. Kumar KS, Sonnemann J, Hong le TT et al (2007) Histone deacetylase inhibitors, but not vincristine, cooperate with radiotherapy to induce cell death in medulloblastoma. Anticancer Res 27:465–470
24. Whelan HT, Krouwer HG, Schmidt MH et al (1998) Current therapy and perspectives in the treatment of Medulloblastoma. Pediatr Neurol 18:103–115. doi:10.1016/S0887-8994(97)00221-X
25. Cervoni L, Cantore G (1995) Medulloblastoma in pediatric age: a single institution review of prognostic factors. Childs Nerv Syst 11:80–85. doi:10.1007/BF00303809
26. Hoppe-Hirsch E, Brunet L, Laroussinie F et al (1995) Intellectual outcome in children whit malignant tumors of the posterior fossa: influence of the field of irradiation and quality of surgery. Childs Nerv Syst 11:340–346. doi:10.1007/BF00301666
27. Dennis M, Spiegler BJ, Htherington CR et al (1996) Neuropsychological sequela of the treatment of children with medulloblastoma in infants. J Neurooncol 29:91–101. doi:10.1007/BF00165522
28. Criswell T, Leskov K, Miyamoto S et al (2003) Transcription factors activated in mammalian cells after clinically relevant doses of ionizing radiation. Oncogene 22:5813–5827. doi:10.1038/sj.onc.1206680
29. Belka C (2006) The fate of irradiated tumor cells. Oncogene 25:969–970. doi:10.1038/sj.onc.1209175
30. Gudkov AV, Komarova EA (2003) The role of p53 in determining sensitivity to radiotherapy. Nat Rev Cancer 3:117–129. doi:10.1038/nrc992
31. Willers H, Dahm-Daphi J, Powell SN (2004) Repair of radiation damage to DNA. Br J Cancer 90:1297–1301. doi:10.1038/sj.bjc.6601729
32. Zhou BB, Elledge SJ (2000) The DNA damage response: putting checkpoints in perspective. Nature 408:433–439. doi:10.1038/35044005
33. Niida H, Nakanishi M (2006) DNA damage checkpoints in mammals. Mutagenesis 21:3–9. doi:10.1093/mutage/gei063
34. Perry ME (2004) MDM2 in response to radiation. Mol Cancer Res 2:9–19
35. Chang BD, Broude EV, Dokmanovic M et al (1999) A senescence-like phenotype distinguishes tumor cells that undergo terminal proliferation arrest after exposure to anticancer agents. Cancer Res 59:3761–3767
36. Kemp CJ, Sun S, Gurley KE (2001) p53 induction and apoptosis in response to radio- and chemotherapy in vivo is tumor-type-dependent. Cancer Res 61:327–332
37. Roninson IB, Broude EV, Chang BD (2001) If not apoptosis, then what? Treatment-induced senescence and mitotic catastrophe in tumor cells. Drug Resist Update 4:303–313. doi:10.1054/drup. 2001.0213
38. Gottardo NG, Gajjar A (2006) Current therapy for medulloblastoma. Curr Treat Options Neurol 8:319–334. doi:10.1007/s11940-006-0022-x
39. Oren M (2003) Decision making by p53: life, death and cancer. Cell Death Differ 10:431–442. doi:10.1038/sj.cdd.4401183
40. Appella E, Anderson CW (2001) Post-translational modifications and activation of p53 by genotoxic stresses. Eur J Biochem 268:2764–2772. doi:10.1046/j.1432-1327.2001.02225.x
41. Maya R, Balass M, Kim ST et al (2001) ATM-dependent phosphorylation of Mdm2 on serine 395: role in p53 activation by DNA damage. Genes Dev 15:1067–1077. doi:10.1101/gad.886901
42. Offer H, Erez N, Zurer I et al (2002) The onset of p53-dependent DNA repair or apoptosis is determined by the level of accumulated damaged DNA. Carcinogenesis 23:1025–1032. doi:10.1093/carcin/23.6.1025
43. Frank AJ, Hernan R, Hollander A et al (2004) The TP53-ARF tumor suppressor pathway is frequently disrupted in large/cell anaplastic medulloblastoma. Brain Res Mol Brain Res 121:137–140. doi:10.1016/j.molbrainres.2003.11.016
44. Li Y, He L, Bruce A et al (2006) p14ARF inhibits the growth of p53 deficient cells in a cell-specific manner. Biochim Biophys Acta 1763:787–796. doi:10.1016/j.bbamcr.2006.04.011
45. Iwai A, Marusawa H, Matsuzawa S et al (2004) Siah-1L, a novel transcript variant belonging to the human S family of proteins, regulates beta catenin activity in a p53-dependent manner. Oncogene 23:7593–7560. doi:10.1038/sj.onc.1208016
46. Sadot E, Geiger B, Oren M et al (2001) Down-regulation of beta-catenin by activated p53. Mol Cell Biol 21:6768–6781. doi:10.1128/MCB.21.20.6768-6781.2001
47. Jüllig M, Zhang WV, Ferreira A et al (2006) MG132 induced apoptosis is associated with p53-independent induction of pro-apoptotic Noxa and transcriptional activity of beta-catenin. Apoptosis 11:627–641. doi:10.1007/s10495-006-4990-9
48. van Gijn ME, Snel F, Cleutjens JP et al (2001) Overexpression of components of the Frizzled-Dishevelled cascade results in apoptotic cell death, mediated by beta-catenin. Exp Cell Res 265:46–53. doi:10.1006/excr.2001.5174
49. Tell S, Yi H, Jockovich ME et al (2006) The Wnt signaling pathway has tumor suppressor properties in retinoblastoma. Biochem Biophys Res Commun 349:261–269. doi:10.1016/j.bbrc.2006.08.044
50. Kim K, Pang KM, Evans M et al (2000) Overexpression of beta-catenin induces apoptosis independent of its transactivation function with LEF-1 or the involvement of major G1 cell cycle regulators. Mol Biol Cell 11:3509–3523
51. Olmeda D, Castel S, Vilaro S et al (2003) β-catenin regulation during the cell cycle: implications in G2/M and apoptosis. Mol Biol Cell 14:2844–2860. doi:10.1091/mbc.E03-01-0865
52. Abramova MV, Pospelova TV, Nikulenkov FP et al (2006) G1/S arrest induced by histone deacetylase inhibitor sodium butyrate in E1A + Ras-transformed cells is mediated through down-regulation of E2F activity and stabilization of beta-catenin. J Biol Chem 281:21040–21051. doi:10.1074/jbc.M511059200
53. Damalas A, Kahan S, Shtutman M et al (2001) Deregulated beta-catenin induces a p53- and ARF-dependent growth arrest and cooperates with Ras in trasformation. EMBO J 20:4912–4922. doi:10.1093/emboj/20.17.4912